

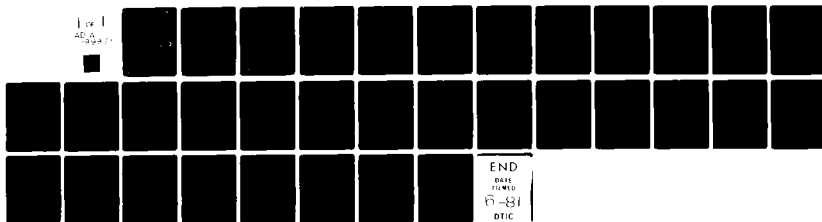
AD-A099 971

NATIONAL BUREAU OF STANDARDS WASHINGTON DC SURFACE S-ETC F/8 7/3  
SURFACE BINDING OF AN ELECTRONIC ANALOG TO CO: INFRARED EVIDENC--ETC(U)  
MAY 81 R R CAVANAGH, J T YATES N00014-81-F-0008  
NL

UNCLASSIFIED

TR-23

1 of 1  
AD-A  
image



END  
DATE  
FILMED  
6-81  
DTIC

AD A099971

① LEVEL II

OFFICE OF NAVAL RESEARCH  
Contract N0014-81-F-0008  
0

Technical Report #23

⑥ Surface Binding of an Electronic Analog to CO: Infrared  
Evidence for  $\text{CH}_3\text{NC}$  Chemisorption on  $\text{Rh}/\text{Al}_2\text{O}_3$ .

⑩ R. R. Cavanagh J. T. Yates, Jr.

(9) *Technical Report*  
Surface Science Division  
National Bureau of Standards  
Washington, DC 20234

② 34

⑪ May 81

DTIC  
ELECTE  
JUN 10 1981  
S B D

⑭ TR-23

⑮ N00014-81-F-0008

Reproduction in whole or in part is permitted for any purpose  
of the United States Government

Approved for Public Release; Distribution Unlimited

To be published in Journal of Chemical Physics

410655

81 6 05 02.6

DTIC FILE COPY

REPORT DOCUMENTATION PAGE		READ INSTRUCTIONS BEFORE COMPLETING FORM
1. REPORT NUMBER Technical Report No. 23✓	2. GOVT ACCESSION NO. AD-A099971	3. RECIPIENT'S CATALOG NUMBER
4. TITLE (and Subtitle) Surface Binding of an Electronic Analog to CO: Infrared Evidence for CH <sub>3</sub> NC Chemisorption on Rh/Al <sub>2</sub> O <sub>3</sub>		5. TYPE OF REPORT & PERIOD COVERED
7. AUTHOR(s) R. R. Cavanagh and J. T. Yates, Jr.		6. PERFORMING ORG. REPORT NUMBER
9. PERFORMING ORGANIZATION NAME AND ADDRESS Surface Science Division National Bureau of Standards Washington, DC 20234		8. CONTRACT OR GRANT NUMBER(s) N0014-81-F-0008✓ Mod. No. P00001
11. CONTROLLING OFFICE NAME AND ADDRESS		10. PROGRAM ELEMENT, PROJECT, TASK AREA & WORK UNIT NUMBERS
14. MONITORING AGENCY NAME & ADDRESS (if different from Controlling Office)		12. REPORT DATE May, 1981
		13. NUMBER OF PAGES
		15. SECURITY CLASS. (of this report) Unclassified
		15a. DECLASSIFICATION/DOWNGRADING SCHEDULE
16. DISTRIBUTION STATEMENT (of this Report)  Approved for Public Release; Distribution Unlimited		
17. DISTRIBUTION STATEMENT (of the abstract entered in Block 20, if different from Report)		
18. SUPPLEMENTARY NOTES  To be published in Journal of Chemical Physics		
19. KEY WORDS (Continue on reverse side if necessary and identify by block number)  Carbon monoxide; chemisorption; infrared spectroscopy; methyl isocyanide; rhodium.		
20. ABSTRACT (Continue on reverse side if necessary and identify by block number)  The chemisorption of methyl isocyanide by Al <sub>2</sub> O <sub>3</sub> supported Rh has been investigated using transmission infrared spectroscopy. Evidence for the absence of dissociation or isomerization upon chemisorption is presented. The identification of various surface binding sites is possible and is in agreement with the site distribution previously demonstrated for such samples using CO with methyl isocyanide. Samples which are exposed to methyl isocyanide following saturation coverage with CO exhibit a 100 cm <sup>-1</sup> decrease in the C≡O (continued on reverse side)		

stretching mode due to the presence of the isocyanide. This shift is interpreted in terms of a  $\sigma$  donor- $\pi^*$  acceptor interaction between the isocyanide and CO adsorbates.

Accession For	
NTIS GRA&I	<input checked="checked" type="checkbox"/>
DTIC TAB	<input type="checkbox"/>
Unannounced	<input type="checkbox"/>
Justification	
By	
Distribution/	
Availability Codes	
Dist	Avail and/or Special
A	

#23

MAR - 9 '81

SURFACE BINDING OF AN ELECTRONIC ANALOG TO CO:  
INFRARED EVIDENCE FOR  $\text{CH}_3\text{NC}$  CHEMISORPTION ON  $\text{Rh}/\text{Al}_2\text{O}_3$

R. R. Cavanagh\* and J. T. Yates, Jr.

Surface Science Division

National Bureau of Standards

Washington, D.C. 20234

\*NRC-NBS Postdoctoral Research

Associate 1979 - 1981

# Abstract

Al<sub>2</sub>O<sub>3</sub>-supported

The chemisorption of methyl isocyanide by Al<sub>2</sub>O<sub>3</sub>-supported Rh has been investigated using transmission infrared spectroscopy. Evidence for the absence of dissociation or isomerization upon chemisorption is presented. The identification of various surface binding sites is possible and is in agreement with the site distribution previously demonstrated for such samples using CO with methyl isocyanide. Samples which are exposed to methyl isocyanide following saturation coverage with CO exhibit a 100/cm<sup>-1</sup> decrease in the C≡O stretching mode due to the presence of the isocyanide. This shift is interpreted in terms of a  $\sigma$  donor- $\pi^*$  acceptor interaction between the isocyanide and CO adsorbates.

$\sigma$  donor- $\pi^*$  acceptor

$\pi$ -back-bonding

## i. Introduction

The analogy between surface chemistry and inorganic chemistry has become the subject of significant speculation in the recent literature.<sup>(1-5)</sup> The potential for transferring the well established behavior of inorganic reactions to the comparatively unexplored field of surface chemistry is very exciting. However, while correlations of chemical reactivity with molecular structure and bonding in inorganic chemistry have been widely established from crystallographic, spectroscopic, and product analysis studies, the extent to which the same structure and bonding concepts can be applied to surface chemistry problems has not been fully demonstrated. For instance, inorganic chemists have examined a variety of metal carbonyls and have extended this work to other ligands including the isocyanides.<sup>(6-8)</sup> Consequently, the similarities and differences between CO and isocyanide ligands have been well studied in the realm of inorganic chemistry and reflect the character of the ligand molecular orbitals in each case. On the other hand, while surface studies of CO binding to various bulk metals and supported systems are interpreted in terms of model inorganic compounds, the analogy of the behavior of CO to the electronically similar isocyanide ligand has rarely been investigated on surfaces. The similarities and differences between CO and  $\text{CH}_3\text{NC}$  can be readily appreciated by examining their molecular orbitals shown in Figure 1.<sup>(9)</sup> The highest occupied molecular orbitals are  $\sigma$  type non-bonding orbitals in each case. The lowest lying unoccupied orbitals are  $\pi^*$  type orbitals in each case. Consequently, the chemistries of the two molecules might be anticipated to mimic one another. However, the absolute binding energies are significantly different, the orbitals being less tightly bound by 4.76 eV and the  $\pi^*$  orbital being higher in energy by 6.71 eV in  $\text{CH}_3\text{NC}$  compared to CO. Consequently,  $\text{CH}_3\text{NC}$  is a far better  $\sigma$  electron donor and a worse  $\pi$  electron

acceptor than CO. The aim of this work is to explore the extension of such analogies to chemical binding at surfaces.

While some early reports have appeared which dealt with isocyanide binding at metal surfaces,<sup>(10)</sup> more recent publications have indicated that dissociation and isomerization processes may be significant.<sup>(11)</sup> We have employed transmission infrared spectroscopy to examine such interactions in a model system. Specifically we report the interaction of  $\text{CH}_3\text{NC}$  with rhodium supported on  $\text{Al}_2\text{O}_3$ . The metal site distribution and CO chemisorption in this system are somewhat controversial but have been well documented.<sup>(12)</sup>

## II. Experimental

The preparation of dispersed samples of Rh on  $\text{Al}_2\text{O}_3$  (Degussa-C and Alon-C)\* has been described previously.<sup>(12,13)</sup> Briefly, a suspension of  $\text{RhCl}_3 \cdot 3\text{H}_2\text{O}$ ,  $\text{Al}_2\text{O}_3$ , water, and acetone is sprayed onto a  $\text{CaF}_2$  or  $\text{BaF}_2$  sample plate which is held at 350K. This procedure flash evaporates the solvents, leaving  $\text{Rh}^{\text{III}}$  ions adsorbed on  $\text{Al}_2\text{O}_3$ . The sample plates were subsequently mounted on a copper support assembly inside a stainless steel 2.75 inch diameter double sided flange equipped with  $\text{CaF}_2$  or  $\text{BaF}_2$  windows. In order to maintain a hydrocarbon free sample, an all metal ultra high vacuum (UHV) manifold was used. Evacuation was accomplished by means of a liquid nitrogen cooled zeolite trap and an ion pump. The ultimate pressure of the system is  $<10^{-8}$  Torr. The evacuated cell is heated to 425K and exposed to  $400 \text{ cm}^3$  of hydrogen at 300 Torr in order to reduce the supported  $\text{Rh}^{\text{III}}$  ions. After three such exposures, the cell is evacuated to  $\sim 10^{-7}$  Torr at 450K for 8 hours and then allowed to cool. Surface areas of such samples have been measured by the BET method giving  $55 \text{ m}^2/\text{gm}$ .<sup>(12)</sup> Typically, 2.2% Rh by weight samples were prepared with a total mass per unit area of  $17 \text{ mg}/\text{cm}^2$ . The loadings for the 10.0% Rh samples were limited to  $4 \text{ mg}/\text{cm}^2$  to avoid total absorbance of the incident infrared beam near  $2200 \text{ cm}^{-1}$  upon exposure to  $\text{CH}_3\text{NC}$ , while the 0.2% samples were limited to  $17 \text{ mg}/\text{cm}^2$  to avoid excessive light scattering due to the  $\text{Al}_2\text{O}_3$ .

A cell design which affords excellent temperature regulation between 100K and 300K has been developed as shown in Figure 2. The cell consists of a standard UHV 2.75 inch body which has ports for gas addition and thermocouple feedthroughs. As in previous designs, the sample is mounted in a copper ring within the cell body. The sample temperature can be adjusted by passing nitrogen gas through the tube brazed to the copper sample support. Temperature regulation is attained by cooling the nitrogen gas and regulating its flow rate through the copper support. Temperature variation of less than  $\pm 3K$  can be maintained for several hours by careful attention to the flow conditions.

The methyl isocyanide ( $CH_3NC$ ) was prepared using a standard synthetic method involving the dehydration of formamide.<sup>(14)</sup> Its purity was checked by infrared spectroscopy of the gas phase. In order to remove any possible decomposition products the  $CH_3NC$  was evacuated at 77K prior to each use. The methyl isocyanide was stored at liquid nitrogen temperature between experiments.

- In addition to  $CH_3NC$ , control experiments were done using related molecules such as cyanogen, acetonitrile, and hydrogen cyanide. Cyanogen ( $C_2N_2$ ) was obtained from Matheson\* and was used without further purification. The acetonitrile ( $CH_3CN$ ) was obtained from Eastman Kodak\*. This liquid was further purified by several freeze-pump-thaw cycles. Infrared spectra of the vapor did not show any evidence of impurities. HCN was prepared by reaction of KCN with concentrated  $H_2SO_4$  followed by vacuum distillation and collection at 77K. All infrared spectra were obtained using a Perkin Elmer Model 180 spectrometer\*.

### III. Results and Discussion

#### A.) Acetonitrile

In order to distinguish the interaction of  $CH_3CN$  with the  $Al_2O_3$  support from the interaction of the molecule with the Rh sites, a series of experiments were conducted on Rh free  $Al_2O_3$ . The sample was prepared as described in the experimental section except no metal salt was introduced. The same thermal

and hydrogen treatments of the  $\text{Al}_2\text{O}_3$  were carried out to insure representative support conditions. The sample was cooled to 90K and  $1.17 \times 10^{21}$   $\text{CH}_3\text{CN}$  molecules per gram of  $\text{Al}_2\text{O}_3$  were introduced into the cell (Figure 3Aa). Figure 3A shows the spectral development as this sample was warmed. From 90K until 175K there is no discernible development of spectral features. At 175K, however, there are distinct features at 2935, 2294, 2254, and  $2215 \text{ cm}^{-1}$ . As the sample was warmed to 230K additional features at 2995, 2330, 1440, and  $1372 \text{ cm}^{-1}$  became evident. Upon evacuating the sample at room temperature, similar spectra to that observed at 230K were obtained.

The observed changes in spectral distribution are principally due to transport effects as the sample warms. As the  $\text{CH}_3\text{CN}$  is initially introduced, it is frozen onto the coldest parts of the sample support assembly. As the support is warmed, the  $\text{CH}_3\text{CN}$  is able to transfer through the vapor phase to the  $\text{Al}_2\text{O}_3$ . Consequently, as the sample is warmed, more  $\text{CH}_3\text{CN}$  is exposed to the infrared beam, and an increase in absorbance is observed in the spectrum. Upon warming to room temperature, the weakly bound  $\text{CH}_3\text{CN}$  is readily desorbed by evacuation.

A sample containing 2.8% Rh on  $\text{Al}_2\text{O}_3$  was prepared as described in the experimental section. This sample was cooled to 90K and subsequently exposed to  $1.2 \times 10^{21}$   $\text{CH}_3\text{CN}$  molecules per gram of  $\text{Al}_2\text{O}_3$ , or 7  $\text{CH}_3\text{CN}$  molecules per Rh. Figure 3B shows the observed spectrum as a function of sample temperature. Comparison with Table 1 and Figure 3A indicate closely similar spectral development to that observed in the Rh free sample. In each case, a maximum in the spectral intensity occurs at 230K, suggesting a weakly-bound species. Warming either sample to room temperature resulted in a reduction of intensity in the C-H stretch region ( $2995, 2936 \text{ cm}^{-1}$ ), the C N stretch region ( $2332, 2293, 2252 \text{ cm}^{-1}$ ), and the CH bend region ( $1372 \text{ cm}^{-1}$ ). Evacuation of the cell at room temperature caused a further reduction in the observed intensity.

The absence either of infrared features which persist upon evacuation, or the appearance of distinct new spectral features (compared to the Rh free sample), suggests that  $\text{CH}_3\text{CN}$  is not strongly chemisorbed to Rh sites. Additional evidence for this conclusion is presented in section D.

#### B.) Methyl Isocyanide

Figure 4a depicts the spectral features observed prior to  $\text{CH}_3\text{NC}$  chemisorption on Rh free  $\text{Al}_2\text{O}_3$  at 90K. Introduction of approximately  $1.4 \times 10^{21}$   $\text{CH}_3\text{NC}$  molecules per gram of  $\text{Al}_2\text{O}_3$  to the 90K sample results in only one new spectral feature at  $2200 \text{ cm}^{-1}$  as seen in figure 4b. As the sample was warmed, additional intensity appeared in the region between  $3000$  and  $2850 \text{ cm}^{-1}$ . At 140K a distinct feature appears at  $2340 \text{ cm}^{-1}$  which disappears at higher temperature. Once the sample reaches 190K, there is no evidence of the  $2340 \text{ cm}^{-1}$  feature, but new features are apparent at 3010, 2953, 2260, 2212, 2195, and  $2160 \text{ cm}^{-1}$ . The relative intensity of these features changes as the sample is brought to room temperature, but no new absorption features are observed. Evacuation of the sample at room temperature results in a significant decrease in intensity of all features as shown in figure 4g.

Table 1 lists gas phase infrared,<sup>15</sup> liquid Raman,<sup>15</sup> and matrix isolation<sup>16</sup> assignments for the normal modes of  $\text{CH}_3\text{NC}$  monomers. Comparison with the features observed on  $\text{Al}_2\text{O}_3$  is quite good. The exception to this good agreement is the  $2340 \text{ cm}^{-1}$  feature. The transient nature of this species suggests that it may be associated with a comparatively weakly bound state on  $\text{Al}_2\text{O}_3$  relative to the bound state observed at higher temperature.

The most striking feature of this system is the observed spectral development with warming. The generally good agreement between infrared, Raman, and matrix isolation studies with the modes observed in this work suggests that there is only a weak interaction of the adsorbate with the surface. Upon evacuation of the sample at room temperature, a significant decrease in infrared intensity is observed for all features indicating a relatively weak interaction

with  $\text{Al}_2\text{O}_3$ .

A 2.8% Rh/ $\text{Al}_2\text{O}_3$  sample was prepared as described earlier. After cooling the sample to 85K approximately 7  $\text{CH}_3\text{NC}$  molecules per Rh were introduced to the system to assure saturation coverage at room temperature. Figure 5 displays the spectral development as a function of temperature. Two strong features appear and disappear as the sample is warmed from 85K to room temperature. First, a sharp, strong feature appears at  $2340\text{ cm}^{-1}$ . Between the temperature range of 107K and 176K, this feature can be seen to develop and then decay in both this sample and in the Rh free  $\text{Al}_2\text{O}_3$ . A second intense feature appears near  $2160\text{ cm}^{-1}$  as the sample warms, but at 300K, its intensity has diminished. These features at  $2340$  and  $2160\text{ cm}^{-1}$  are evident in both the Rh and the Rh free sample. Upon evacuation at room temperature, however, no features between  $2300$  and  $2000\text{ cm}^{-1}$  are evident in the Rh - free  $\text{Al}_2\text{O}_3$  spectrum while strong absorbance persists in the Rh system. Consequently the two low temperature features which disappear on warming can be attributed to gas phase  $\text{CH}_3\text{NC}$  or  $\text{CH}_3\text{NC}$  interactions with the support rather than  $\text{CH}_3\text{NC}$  bound to Rh.

Aside from these two features, the spectra obtained on the  $\text{Al}_2\text{O}_3$  and the Rh/ $\text{Al}_2\text{O}_3$  show significant differences in intensity and peak locations. Table 1 lists the room temperature line positions and the associated normal modes. The relative peak heights in the CH regions suggest that the chemical nature of the methyl groups has not been altered significantly by the presence of the Rh. However, the additional intensity observed at room temperature for the evacuated Rh sample compared to the metal-free  $\text{Al}_2\text{O}_3$  indicates that additional more strongly bound chemisorbed species exist on the Rh compared to the  $\text{Al}_2\text{O}_3$  support.

Samples containing 0.2%, 2.2%, and 10.0% Rh/ $\text{Al}_2\text{O}_3$  were prepared and subsequently saturated with  $\text{CH}_3\text{NC}$ . The spectra in Figure 6 show the C-N features observed between  $2300$  and  $2100\text{ cm}^{-1}$  over a fifty fold range of Rh loading on

$\text{Al}_2\text{O}_3$ . The observed systematic variation of relative intensity is due to the different distribution of metal sites in the samples<sup>(17)</sup>. The features at 2250 and 2190  $\text{cm}^{-1}$  dominate this region of the spectrum as the metal content of the sample is reduced. The feature at 2160  $\text{cm}^{-1}$  becomes more pronounced as the metal loading is increased.

Figure 7 displays the spectral features observed between 3050 and 2800  $\text{cm}^{-1}$ . Once again, metal dispersion is seen to have a marked effect on the observed spectral features. The increased intensity near 2975 and 2929  $\text{cm}^{-1}$  on the 10% Rh samples suggests that these features are due to  $\text{CH}_3\text{NC}$  interaction with crystallite Rh sites. The features near 3010 and 2945  $\text{cm}^{-1}$  are assigned to the corresponding modes in  $\text{CH}_3\text{NC}$  bound to isolated Rh sites. In order to more clearly compare the spectral distributions observed in Figures 7A and 7B, a difference spectrum was generated. Comparison with spectra obtained on 0.2% Rh samples indicated that the feature at 2945  $\text{cm}^{-1}$  is clearly associated with the isolated Rh atoms. Consequently, spectra 7A and 7B were normalized to the same absorbance for this isolated Rh feature at 2945  $\text{cm}^{-1}$ . The contribution due to isolated Rh sites was then removed from the 10% sample by subtraction of the normalized 2.8% spectrum. This procedure involving only 2% Rh and 10% Rh was necessary due to the increasing significance of adsorbed  $\text{CH}_3\text{NC}$  on the  $\text{Al}_2\text{O}_3$  in the data obtained on the 0.2% Rh/ $\text{Al}_2\text{O}_3$ .

Figure 8 displays the variation in the spectral features observed in the CH bending region at various Rh loadings. In each case, two distinct features are observed at 1417 and 1447  $\text{cm}^{-1}$ . In addition, there is a feature below 1400  $\text{cm}^{-1}$ . However, the lack of pronounced spectral changes and the limited signal to noise ratio do not permit the association of these features with distinct metal sites. The site specific assignments are summarized in Table 2.

The potential for dissociative chemisorption of methyl isocyanide on Rh was addressed in a series of experiments. The first experiment used  $\text{BaF}_2$  instead of  $\text{CaF}_2$  for the cell windows and the sample plate. The use of  $\text{BaF}_2$

allowed spectra to be recorded near the transmission limit of the  $\text{Al}_2\text{O}_3$ . Observation on a 2.2% Rh sample indicates a systematic increase in absorbance below  $940\text{ cm}^{-1}$  as  $\text{CH}_3\text{NC}$  was adsorbed at 300K. This corresponds to the CN single bond stretch mode, indicating that the  $\text{H}_3\text{C-N}$  bond is still intact. Unfortunately, strong absorbance due to the  $\text{Al}_2\text{O}_3$  below  $930\text{ cm}^{-1}$  would not permit the observation of a local maximum in the absorbance in this region.

C.) Attempts to Produce Chemisorbed CN on Rh.

In two separate experiments, an attempt was made to generate surface  $\text{C}\equiv\text{N}$  groups. In one case, since cyanogen is thought to dissociate on platinum,<sup>(18,19)</sup> a 2.2% rhodium sample was saturated with  $(\text{CN})_2$  at 300K in order to investigate the potential of dissociative chemisorption in this system. The only infrared spectral features which were observed were weak, occurring at 2298, 2157, and  $2105\text{ cm}^{-1}$ . Subsequent exposure to CO resulted in an unperturbed spectrum for CO chemisorbed on rhodium. The lack of strong spectral features combined with a preserved activity for CO chemisorption (see section D) is indicative that the surface species due to cyanogen is significantly different from that due to  $\text{CH}_3\text{NC}$ .

In a second experiment, a 2.2% Rh sample was exposed to HCN in a further effort to generate Rh-CN,<sup>(20-22)</sup>. Additional intensity was observed between  $3500$  and  $2700\text{ cm}^{-1}$  and between  $2180$  and  $2000\text{ cm}^{-1}$ , which probably correspond to molecular HCN modes<sup>(15)</sup> at  $3312$  and  $2089\text{ cm}^{-1}$ . No additional features were observed. Exposure of the HCN-saturated sample to CO resulted in an unperturbed spectrum of chemisorbed CO.

Cyanogen and hydrogen cyanide are excellent candidates for possible production of surface CN groups on Rh. The absence of pronounced spectral features corresponding to surface  $\text{-C}\equiv\text{N}$  in these experiments, is to be contrasted with the strong features observed in the isocyanide case. Consequently, the spectral features observed for  $\text{CH}_3\text{NC}$  are consistent with non-dissociative

chemisorption on Rh.

In the  $(\text{CN})_2$  and HCN experiments, the corresponding, rhodium-free samples were not examined. Consequently, the contributions due to species on the  $\text{Al}_2\text{O}_3$  are not clear. There is no doubt, however, that comparable  $\text{C}\equiv\text{N}$  stretching features to those seen with  $\text{CH}_3\text{NC}$  do not exist in either the  $(\text{CN})_2$  or HCN experiments. Therefore, irrespective of the precise nature of the adsorbate species produced and the binding sites involved (i.e., binding to metal sites compared to support sites), the distinctly different spectral and chemical behavior of these systems compared to that observed for  $\text{CH}_3\text{NC}$  is well demonstrated.

#### D.) Interactions with CO

In order to measure the relative binding strengths of acetonitrile,  $\text{CH}_3\text{CN}$ , on the Rh sites, CO was introduced to a sample following a saturation exposure of  $\text{CH}_3\text{CN}$ . Figure 9 shows the development of strong features at 2101, 2068, 2027, and  $1875\text{ cm}^{-1}$ , indicative of CO chemisorption on clean  $\text{Rh}/\text{Al}_2\text{O}_3$ <sup>(12)</sup>. This observation confirms the lack of a strong chemical interaction between  $\text{CH}_3\text{CN}$  and Rh. A similar CO adsorption experiment was carried out on a Rh surface saturated with  $\text{CH}_3\text{NC}$  at 300K. In this case, no significant changes following exposure to CO were observed. Neither the appearance of new features attributable to CO, nor alteration of existing  $\text{CH}_3\text{NC}$  peaks was observed. The difference in the CO binding of these two preadsorbed samples further demonstrates the distinct difference in binding of acetonitrile compared to methyl isocyanide.

A test of the relative binding strengths of CO and  $\text{CH}_3\text{NC}$  was made in the following experiment. A 2.2%  $\text{Rh}/\text{Al}_2\text{O}_3$  sample was prepared and subsequently saturated with  $^{13}\text{CO}$ . This sample was then exposed to a series of  $\text{CH}_3^{13}\text{NC}$  doses at 300K. The sequential interaction of  $\text{CH}_3^{13}\text{NC}$  with CO is shown in Figure 10. At full coverage, the  $\text{CH}_3^{13}\text{NC}$  features have grown in, apparently unperturbed by the CO in the system. It can also be seen that the CO doublet

is systematically eliminated by the adsorption of  $\text{CH}_3\text{NC}$ . However, the bridging CO feature at  $1840\text{ cm}^{-1}$  remains during the experiment, and systematically shifts down by  $\sim 100\text{ cm}^{-1}$ . An additional feature also appears at  $1930\text{ cm}^{-1}$  in spectrum (c) and shifts down in wave number with increasing coverage of  $\text{CH}_3\text{NC}$ . The identity of these two features which appear below  $2000\text{ cm}^{-1}$  was determined by a gas phase exchange of the residual  $^{13}\text{CO}$  on the sample with  $^{12}\text{CO}(\text{g})$ . This experiment is illustrated in Figure 11. Following  $^{12}\text{CO}$ -exchange, the two peaks below  $2000\text{ cm}^{-1}$  are both observed to shift to higher wave number by approximately  $40\text{ cm}^{-1}$ , while the remaining spectral features are unaffected. This clearly identifies the two peaks in question as being due to CO chemisorbed on Rh and perturbed by subsequent  $\text{CH}_3\text{NC}$  chemisorption.

It is interesting to note that the two CO features observed can both be seen to gradually shift to lower wave number as  $\text{CH}_3\text{NC}$  is introduced. These two features have both previously been assigned, one as linear CO on Rh crystallites and the other as CO in a bridge site on Rh crystallites<sup>(12)</sup>. Consequently, the  $\text{CH}_3\text{NC}$  can be seen to be associated with a net shift to lower wave number of both of these features by  $100\text{ cm}^{-1}$ . There is no spectral evidence for isolated Rh sites which simultaneously bind CO and  $\text{CH}_3\text{NC}$ .

#### IV. Conclusions

##### A.) Absence of Catalytic Isomerization of $\text{CH}_3\text{NC}$ to $\text{CH}_3\text{CN}$ on Rh.

The gas phase isomerization of  $\text{CH}_3\text{NC}$  to  $\text{CH}_3\text{CN}$  is a well known process.<sup>(23)</sup> As an exothermic reaction ( $\Delta H=63\text{ kJoule/mole}$ ) with a moderate activation energy ( $E_a=161\text{ kJoule/mole}$ ), the potential for a surface-induced isomerization at 300K seems considerable. However, distinctly different spectra were obtained in the  $\text{CH}_3\text{NC}$  and the  $\text{CH}_3\text{CN}$  adsorption experiments. The observed frequencies of the C-N mode, the relative stability during evacuation, and the capacity to block CO binding sites all indicate significantly different

chemistries for the two adsorbates. The absence of  $\text{CH}_3\text{NC}$  isomerization on Rh is therefore unambiguous. This lack of conversion to the thermodynamically more stable form provides compelling evidence that the analogy between inorganic chemistry and surface chemistry is substantive. The recognized stability towards isomerization of isocyanides in model inorganic complexes suggests a non-isomerizing surface interaction. The lack of isomerization which has been clearly demonstrated in this work illustrates that similar chemistry occurs on the metal surface and in well-known inorganic compounds.

B.) Evidence for Non-Dissociative  $\text{CH}_3\text{NC}$  chemisorption on Rh.

The question of dissociative chemisorption of  $\text{CH}_3\text{NC}$  is more difficult to address. However, our results from three different experiments all argue for the absence of dissociative processes. In brief: a) observation of absorbance in the region expected for the  $\text{N-CH}_3$  stretch is indicative of lack of dissociation; b) chemisorption of  $(\text{CN})_2$  or HCN does not result in any features comparable to those observed with  $\text{CH}_3\text{NC}$ .

Comparison of these results with earlier data is interesting. For  $\text{CH}_3\text{CH}_2\text{NC}$  chemisorbed on rhodium films, similar results to those obtained in this work were reported on the basis of limited spectroscopic evidence<sup>(10)</sup>. At that time, however, no evidence was available to demonstrate the absence of either isomerization or dissociation of the isocyanide. Based on the present work, it is clear that the original interpretation presented<sup>(10)</sup> is valid. It is more difficult to make comparison with the recent work on single crystals.<sup>(11,24)</sup> While significantly different surface interactions were suggested on bulk nickel, the variation in reactivity between nickel compared to rhodium is well known. In addition a non dissociative low temperature state of  $\text{CH}_3\text{NC}$  was identified on Fe(110), using ultraviolet photoelectron spectroscopy. This species showed evidence of decomposition upon warming to 470K.<sup>(24)</sup> Furthermore, there may

be subtle differences between the interaction of  $\text{CH}_3\text{NC}$  with bulk metals compared to behavior observed on dispersed samples of the same material.<sup>(25)</sup> Consequently, detailed comparison will not be possible until dispersed nickel or bulk rhodium studies are completed.

#### C.) Surface Binding of Methyl Isocyanide to Rhodium

The observed IR spectral features can be attributed to a combination of features due to  $\text{CH}_3\text{NC}$  chemisorbed on isolated Rh sites and on Rh crystallites. Table 2 indicates assignments for the two types of sites where a distinction was possible. It is interesting to note that in comparison to the binding of CO to such samples where two CO ligands are observed per isolated rhodium atom, only one  $\text{N}\equiv\text{C}$  mode is observed for isolated Rh sites. In addition, there is infrared evidence for only one  $\text{CH}_3\text{NC}$  species on the Rh crystallites. By analogy to model inorganic compounds, the  $2160\text{ cm}^{-1}$  crystallite feature can be assigned to linearly bound  $\text{CH}_3\text{NC}$  on Rh crystallites. There is no evidence for bridging  $\text{CH}_3\text{NC}$  which would be expected near  $1800\text{ cm}^{-1}$ . The observation of only one  $\text{N}\equiv\text{C}$  stretching feature for isolated Rh sites could be due to two causes: (a) only one  $\text{CH}_3\text{NC}$  chemisorbs on an isolated Rh site, or (b) two  $\text{C}_3\text{NC}$  groups chemisorb, forming a  $180^\circ$  C-Rh-C bond angle, leading to single infrared active asymmetric  $\text{C}\equiv\text{N}$  stretch mode. On steric grounds, two  $\text{CH}_3\text{NC}$  ligands could readily adsorb at angles significantly less than  $180^\circ$ , as observed in metal isocyanide complexes. Hence we prefer explanation (a) to explain the single  $\text{C}\equiv\text{N}$  infrared feature on the isolated sites.

#### D.) CO - $\text{CH}_3\text{NC}$ adsorbate Interactions.

Distinctions between  $\text{CH}_3\text{NC}$  and CO interactions with the surface are best illustrated by the sequential adsorption experiments. Standard preparative techniques for metal isocyanide complexes involve CO displacement from metal carbonyls, but usually at elevated temperature. The data presented in Figure 10 clearly demonstrate the strong interaction of  $^{13}\text{CO}$  with methyl isocyanide in

this supported system. The progressive disappearance of the 2060-1960  $\text{cm}^{-1}$   $\text{Rh}(\text{}^{13}\text{CO})_2$  doublet as the  $\text{CH}_3\text{NC}$  adsorption spectrum develops demonstrates that the  $\text{Rh}(\text{}^{13}\text{CO})_2$  species are converted to  $\text{RhCNCH}_3$ . The direct displacement corresponds well to the behavior observed in inorganic systems. The persistence of two features between 2100 and 1700  $\text{cm}^{-1}$  indicates that linear and bridged CO on the Rh crystallites are not affected in the same fashion as the  $\text{Rh}(\text{CO})_2$  species. Figure 10 clearly shows that, in the presence of  $\text{CH}_3\text{NC}$ , these CO stretching modes on the crystallites are shifted to lower wave number by 100  $\text{cm}^{-1}$ . The possibility exists that there is some displacement of CO from the crystallite sites during this process. While no substantial change in intensity of the CO features is observed, there may be a simultaneous increase of the CO extinction coefficient due to the interaction with  $\text{CH}_3\text{NC}$ . Therefore, the exact amount of CO remaining on the crystallites cannot be determined in these experiments without a quantitative measurement of the perturbation of the CO extinction coefficients due to interactions with the methyl isocyanide.

The substantial shift in wave number observed for CO in the presence of  $\text{CH}_3\text{NC}$  is not unique. Such shifts in CO stretching modes are known in inorganic systems<sup>(26)</sup> and have been previously reported for  $\text{CH}_3\text{CH}_2\text{NC}$  on rhodium films.<sup>(10)</sup> The effect can be interpreted in terms of an increased back donation to the antibonding  $\pi$  levels of CO in the presence of a good electron donor such as  $\text{CH}_3\text{NC}$ .<sup>(27)</sup> Figure 1 depicts the relative positions of the orbitals for the two molecules. Since the non-bonding  $\sigma$  electrons of the  $\text{CH}_3\text{NC}$  are less tightly bound than those in CO, and since the empty  $\pi$  orbitals are energetically more accessible in CO, the crystalline sites are able to transfer the increased electron density provided by the  $\text{CH}_3\text{NC}$   $\sigma$  orbital back into the CO  $2\pi$  orbitals.

An interesting comparison can be made between studies of CO - CO interactions<sup>(28)</sup> on single crystal surfaces as a function of CO coverage and this work. Bradshaw et. al.<sup>(29)</sup> have shown that the dipole-dipole coupling

between CO adsorbate molecules on Pd(100) is responsible for a coverage dependent shift in  $\nu_{\text{CO}}$  which is of order  $+40 \text{ cm}^{-1}$  as  $\theta_{\text{CO}}$  increases from 0 to 1. Thus a possible interpretation of the  $100 \text{ cm}^{-1}$  shift of  $\nu_{\text{CO}}$  to lower frequency with increased  $\text{CH}_3\text{NC}$  coverage would involve displacement of CO from the crystallites and accompanied reduction in  $\nu_{\text{CO}}$  due only to CO coverage decrease in the CO layer. However, the magnitude of the  $\text{CH}_3\text{NC}$ -induced shift in  $\nu_{\text{CO}}$  is too large to be explained in this manner. A substantial chemical effect between  $\text{CH}_3\text{NC}$  (ads) and CO (ads) on Rh crystallites must be operative as suggested by the molecular orbital arguments.

#### V. Summary

- a.) Non-dissociative binding of  $\text{CH}_3\text{NC}$  to both the isolated Rh atom sites and to the crystalline Rh sites is observed at 300K, in good agreement with the binding observed for CO on these sites.
- b.) No significant isomerization of  $\text{CH}_3\text{NC}$  to the more stable isomer,  $\text{CH}_3\text{CN}$  (acetonitrile) is detectable on Rh/ $\text{Al}_2\text{O}_3$  surfaces.
- c.) Site specific spectral assignments have been made for  $\text{C}\equiv\text{N}$  stretching and C-H stretching modes due to  $\text{CH}_3\text{NC}$  chemisorption on crystalline Rh sites and on isolated Rh atom sites.
- d.) Acetonitrile, cyanogen, and hydrogen cyanide, if bound to the metal sites, are directly displaced by carbon monoxide.
- e.) Methyl isocyanide displaces the CO bound to the isolated Rh sites,  $\text{Rh}(\text{CO})_2$ , without formation of a detectable  $\text{Rh}(\text{CO})(\text{CNCH}_3)$  complex.
- f.) Methyl isocyanide strongly interacts with CO bound to crystalline Rh sites, shifting the two adsorbed CO features  $100 \text{ cm}^{-1}$  to lower energy. This behavior is indicative of a thru metal charge transfer from the isocyanide to the CO.

## Acknowledgements

We acknowledge with thanks partial financial support from the Office of Naval Research.

\* The identification of suppliers of various chemicals and equipment is provided to convey experimental details to the reader. The use of these in no way implies endorsement by the National Bureau of Standards.

## REFERENCES

1. E. L. Muetterties, *Bull, Soc. Chim, Belg.* 84 959 (1975)
2. R. Vgo, *Catal. Rev. - Sci Eng.* 11 225 (1975)
3. R. P. Messmer and K. H. Johnson in Electrocatalysis on Non-Mettallic Surfaces, Spec. Publ. 455 (NBS) Editor, A. D. Franklin.
4. E. L. Muetterties, *Science* 196 839 (1977)
5. A. Brenner and D. A. Hucul, *J. Amer. Chem. Soc.* 102 2484 (1980).
6. L. Malatesta and F. Bonati, Isocyanide Complexes of Metals, Wiley-Interscience, New York 1969.
7. I. Ugi, editor Isonitrile Chemistry, Academic Press, New York, 1971
8. P. M. Treichel, *Advances in Organometallic Chemistry* 11 21 (1973)
9. W. L. Jorgensen and L. Salem The Organic Chemist's Book of Orbitals Academic, New York, 1973.
10. R. Queau and R. Poilblanc, *J. Catalysis* 27 200 (1972).
11. J. C. Hemminger, E. L. Muetterties, and G. A. Somorjai, *J. Amer. Chem. Soc.* 101 62 (1979).
12. J. T. Yates, Jr., T. M. Duncan, S. D. Worley, and R. W. Vaughan, *J. Chem. Phys.* 70, 1219 (1979).
13. J. T. Yates, Jr., T. M. Duncan, and R. W. Vaughan, *J. Chem. Phys.* 71, 3908 (1979).
14. J. Casanova, Jr., R. E. Schuster, and N. D. Wernër, *J. Chem. Soc.* 4380 (1963).
15. G. Herzberg, *Molecular Spectra and Molecular Structure II*, Van Nostrand Reinhold Co. New York, NY (1945).
16. T. B. Freedman and E. R. Nixon, *Spectrochimica ACTA* 28A 1375 (1972).
17. R. R. Cavanagh and J. T. Yates, Jr, Submitted, *J. Chem. Phys.*
18. W. Hoffman, E. Bertel, and F. P. Netzer, *J. of Catalysis* 60 316 (1979).
19. M. E. Bridge and R. M. Lambert, *Surface Science* 63 315 (1977).
20. H. Dunken and H. Hobert, *Z. Chem.* 4, 275 (1964).
21. G. Kortum and H. Delefs, *Spectrochimica ACTA* 20, 405 (1964).
22. M. J. D. Low and P. Ramamurthy, *J. Res. Inst. Catalysis, Hoddaido Univ.* 16, 535 (1968).

23. F. W. Schneider and B. S. Rabinovitch, J. Amer. Chem. Soc. 84 4215 (1962).
24. G. Ertl, J. Kuppers, F. Nitschke, and M. Weiss, Chem. Phys. Lett. 52, 309 (1977).
25. T. S. Kurtikyan and V. T. Aleksanyan, Bull. Acad. Sci USSR 27 1334 (1978).
26. M. Bigorne, J. Organometallic Chemistry 1 101 (1963).
27. F. A. Cotton and F. Zingales, J. Amer. Chem. Soc. 83, 351 (1961).
28. A. Crossley and D. A. King, Surface Science 95, 131 (1980).
29. A. Bradshaw, et. al., private communication.

# FIGURE CAPTIONS

- Figure 1. Carbon Monoxide and Methyl Isocyanide Molecular Orbitals (9).
- Figure 2. Transmission IR cell for supported metals. Vacuum feedthroughs are shown for thermocouples and for circulating coolant.
- Figure 3. Spectral development with increasing temperature for acetonitrile. a) adsorbed  $\text{CH}_3\text{CN}$  at 90K, b-e) subsequent warming. A.) Rh free  $\text{Al}_2\text{O}_3$  B.) 2.8% Rh/ $\text{Al}_2\text{O}_3$
- Figure 4. Spectral development with increasing temperature for methyl isocyanide on Rh free  $\text{Al}_2\text{O}_3$ .
- Figure 5. Development of IR features for 2.8% Rh/ $\text{Al}_2\text{O}_3$  exposed to  $\text{CH}_3\text{NC}$  at 85K and allowed to warm to 310K.
- Figure 6.  $\text{C}\equiv\text{N}$  stretch region of  $\text{CH}_3\text{NC}$  for various Rh loading following background subtraction. A.) 0.2% Rh/ $\text{Al}_2\text{O}_3$ , B.) 2.2% Rh, C.) 10.0% Rh. All spectra were obtained at 300K.
- Figure 7. Infrared spectrum of C-H stretching modes of  $\text{CH}_3\text{NC}$  chemisorbed on Rh following background subtraction. A.) 2.8% Rh, B.) 10% Rh, C.) B-A after normalizing the intensity at  $2945\text{ cm}^{-1}$ .
- Figure 8. Infrared spectrum of C-H bending modes of  $\text{CH}_3\text{NC}$  Chemisorbed on Rh. Three metal loadings of 0.2%, 2.8%, and 10.0% are shown after background subtraction. The broken line below  $1380\text{ cm}^{-1}$  indicates that the signal/background was low.
- Figure 9. A.) Infrared spectrum of  $\text{CH}_3\text{CN}$  on 2.8% Rh/ $\text{Al}_2\text{O}_3$  at 300K. B.) Infrared spectrum obtained after exposing A to CO.
- Figure 10. Infrared spectra showing interactions of chemisorbed CO with  $\text{CH}_3\text{NC}(g)$ . A.) 2.2% Rh sample saturated with  $^{13}\text{CO}$ . B.) and C.) sequential exposure of A to  $\text{CH}_3\text{NC}$ . D.) Saturation coverage of  $\text{CH}_3\text{NC}$  after spectrum C.
- Figure 11. Isotopic exchange of adsorbed CO. A.) Spectrum 10D showing 2.2% Rh/ $\text{Al}_2\text{O}_3$ . B.) Spectrum obtained after exposure of A to 50 Torr. of  $^{12}\text{CO}$  for 10 min. at 300K.

TABLE 1

Vibrational Frequencies for  $\text{CH}_3\text{NC}$  and  $\text{CH}_3\text{CN}$  (in  $\text{cm}^{-1}$ )

$\text{CH}_3\text{NC}$	<u>Gas/Liquid</u> (14)	<u>Matrix</u> (15)	<u><math>\text{Al}_2\text{O}_3</math></u>	<u><math>\text{Rh/Al}_2\text{O}_3</math></u>
$\nu_5$ -C-H asym stretch	3014/3002	3011	3010	2975, 3003 (m)
$\nu_1$ -C-H sym stretch	2965.8/2951	2959	2953	2925, 2946 (m)
$\nu_2$ -N $\equiv$ C stretch	2166/2151	2150.6	(2340)	(2340)
$\nu_6$ - $\text{CH}_3$ deform	1466.9/1456	1457	1455	2160(s), 2199(s), 2251(w)
$\nu_3$ - $\text{CH}_3$ deform	1429/1414	1421.6	1417	1448' (m)
$\nu_4$ -C-N stretch	944.6/928			1415 (s)
				1391
				940
			(2853)	(2883)
				(2861)
			(2814)	(2813)
$\text{CH}_3\text{CN}$	<u>Gas/Liquid</u>	<u>Matrix</u>	<u><math>\text{Al}_2\text{O}_3</math></u>	<u><math>\text{Rh/Al}_2\text{O}_3</math></u>
$\nu_5$ -C-H asym stretch	3009.2/2999	3004	2995	2995
$\nu_1$ -C-H sym stretch	2953.9/2942	2950	2936	2936
$\nu_2$ -C $\equiv$ N stretch	2266.4/2249	2258.4	2230, 2292, 2350	2253, 2293, 2330
$\nu_6$ - $\text{CH}_3$ deform	1448/1440	1445	1400-1450	1440-1450
$\nu_3$ - $\text{CH}_3$ deform	1376/1390	1375.8	1372	1372

TABLE 2  
Spectral Assignments for Specific Rh sites

	<u>Isolated Rh (<math>\text{cm}^{-1}</math>)</u>	<u>Crystallite Rh (<math>\text{cm}^{-1}</math>)</u>
$\nu_5$ -C-H asym stretch	3010 (m)	2975 (m)
$\nu_1$ -C-H sym stretch	2945 (m)	2925 (m)
$\nu_2$ -N $\equiv$ C stretch	2195 (s)	2160 (s)

# Carbon Monoxide and Methyl Isocyanide- Molecular Orbitals

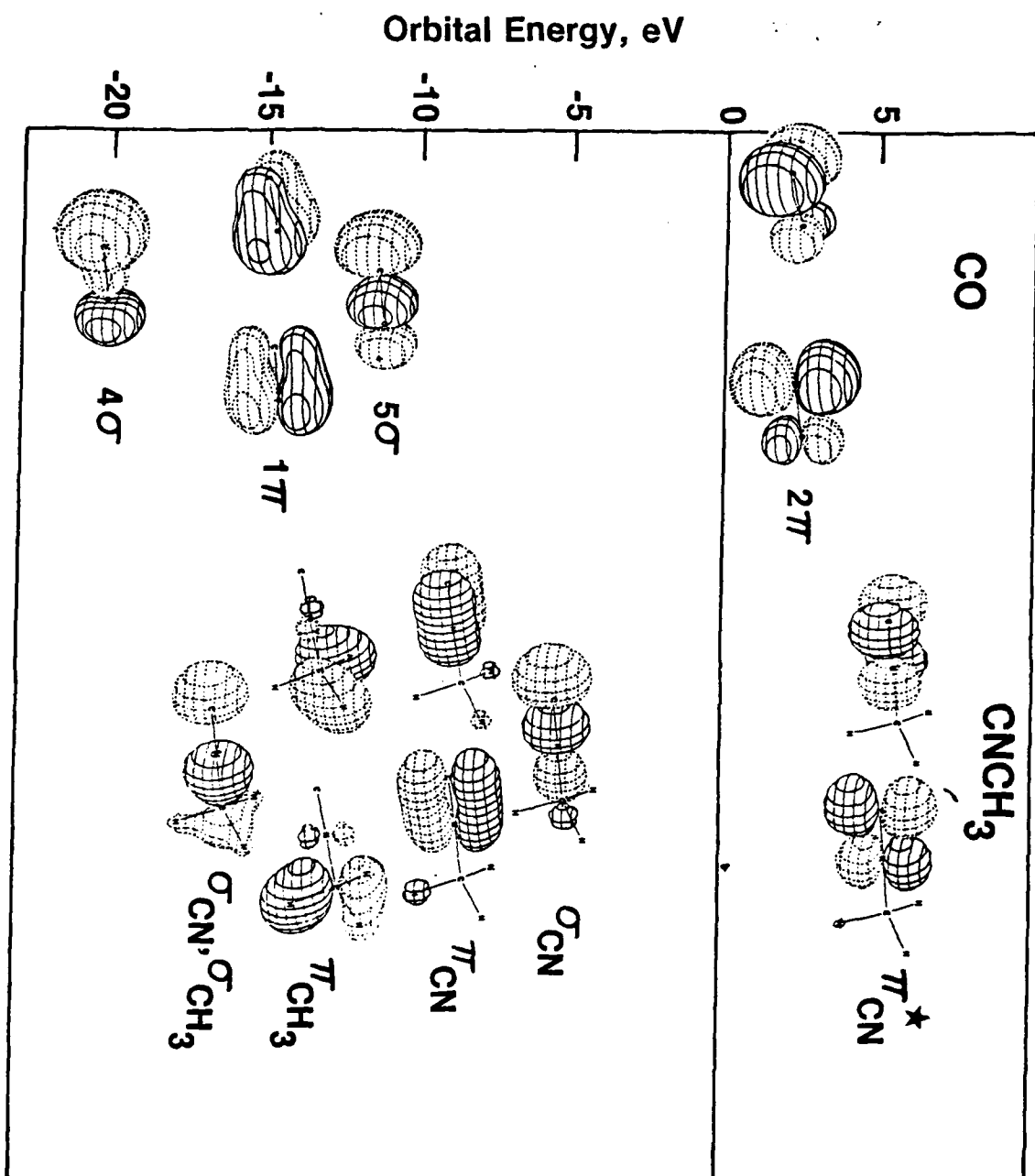


Figure 1

## Variable Temperature Infrared Cell

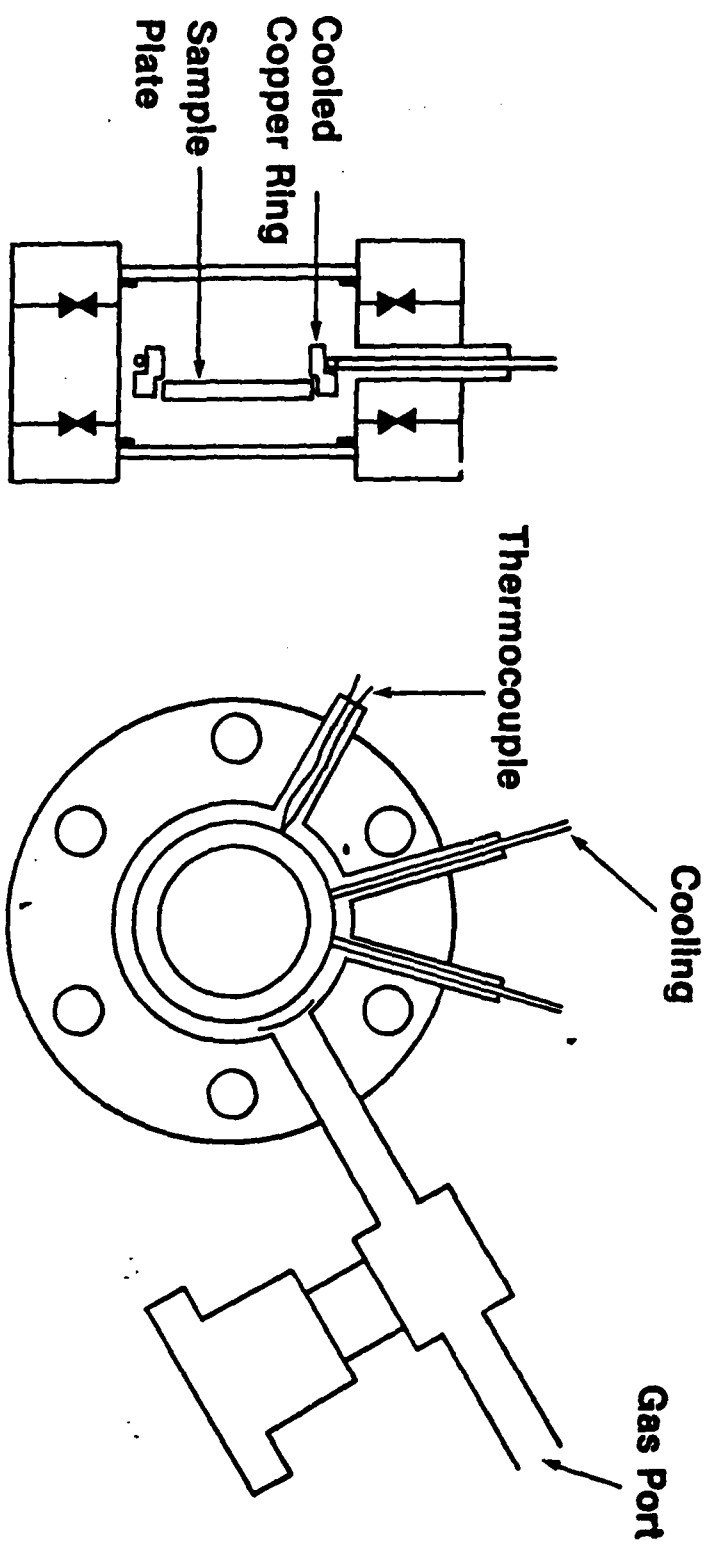


Figure 2

Infrared Spectrum of Chemisorbed  $\text{CH}_3\text{CN}$ :  
 $\text{Al}_2\text{O}_3$  and  $\text{Rh}/\text{Al}_2\text{O}_3$

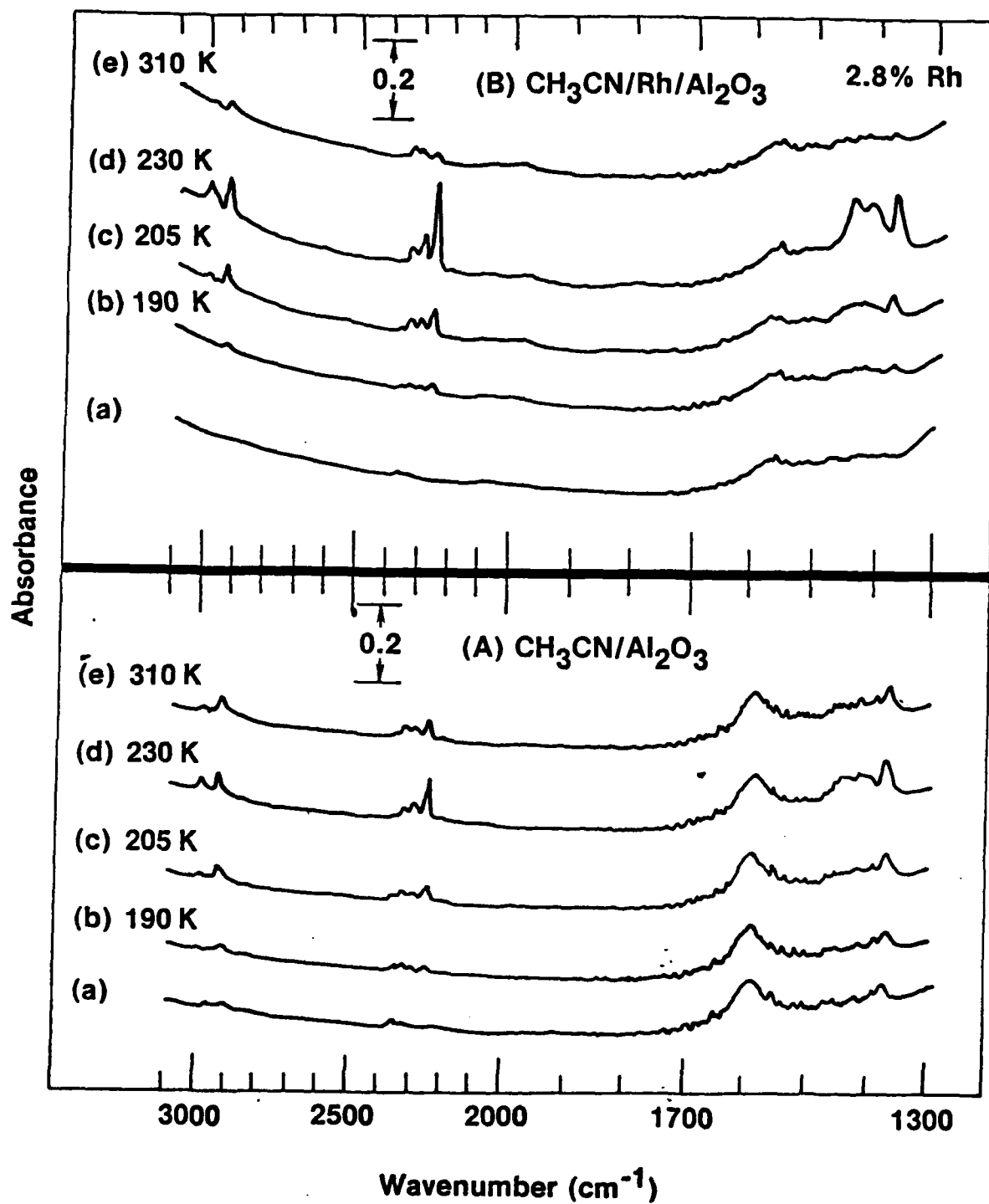


Figure 3

# Infrared Spectrum of $\text{CH}_3\text{NC}$ on $\text{Al}_2\text{O}_3$

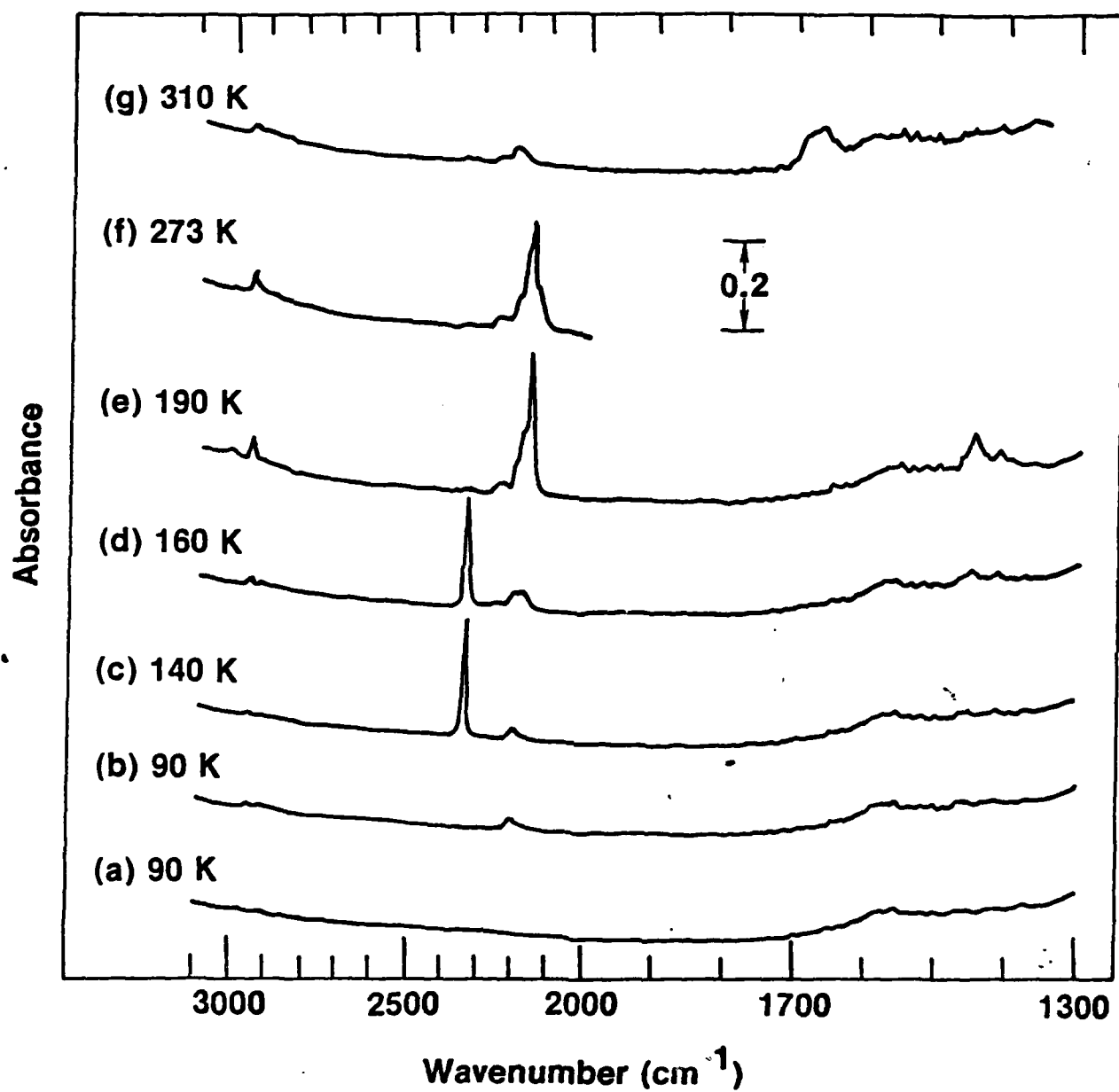


Figure 4

# Infrared Spectrum of $\text{CH}_3\text{NC}$ on $\text{Rh}/\text{Al}_2\text{O}_3$

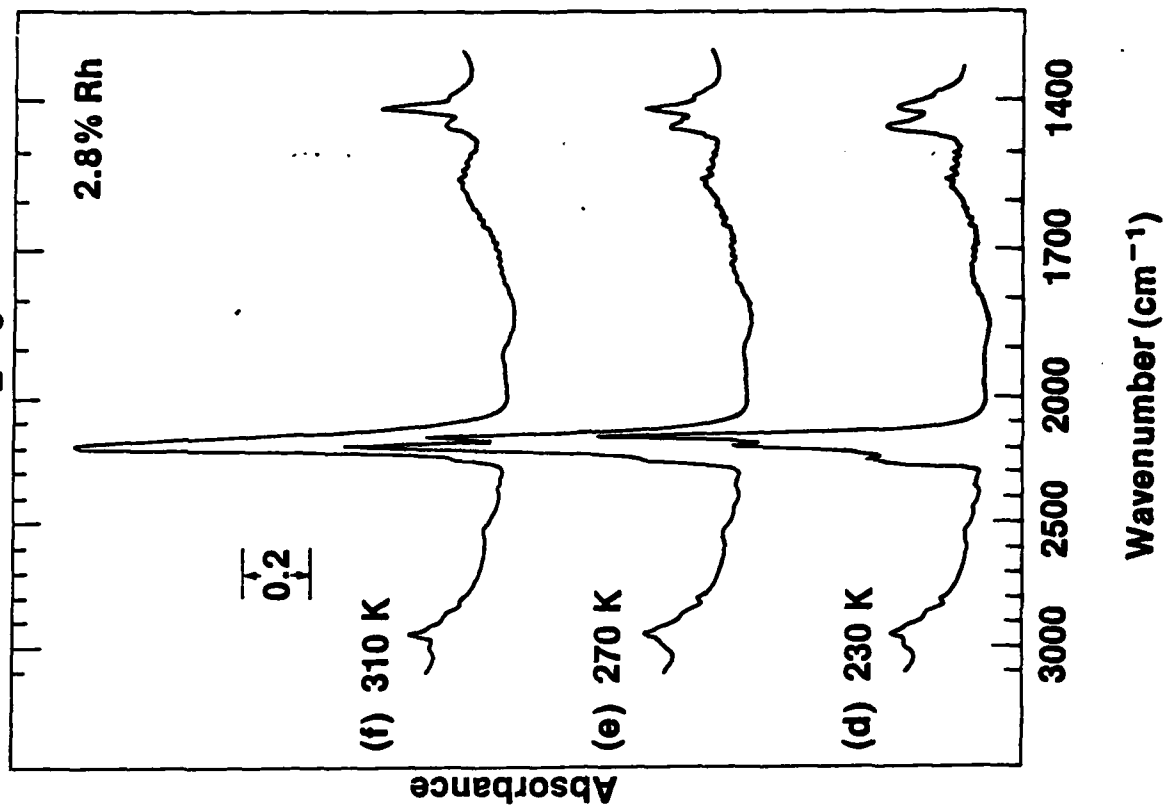
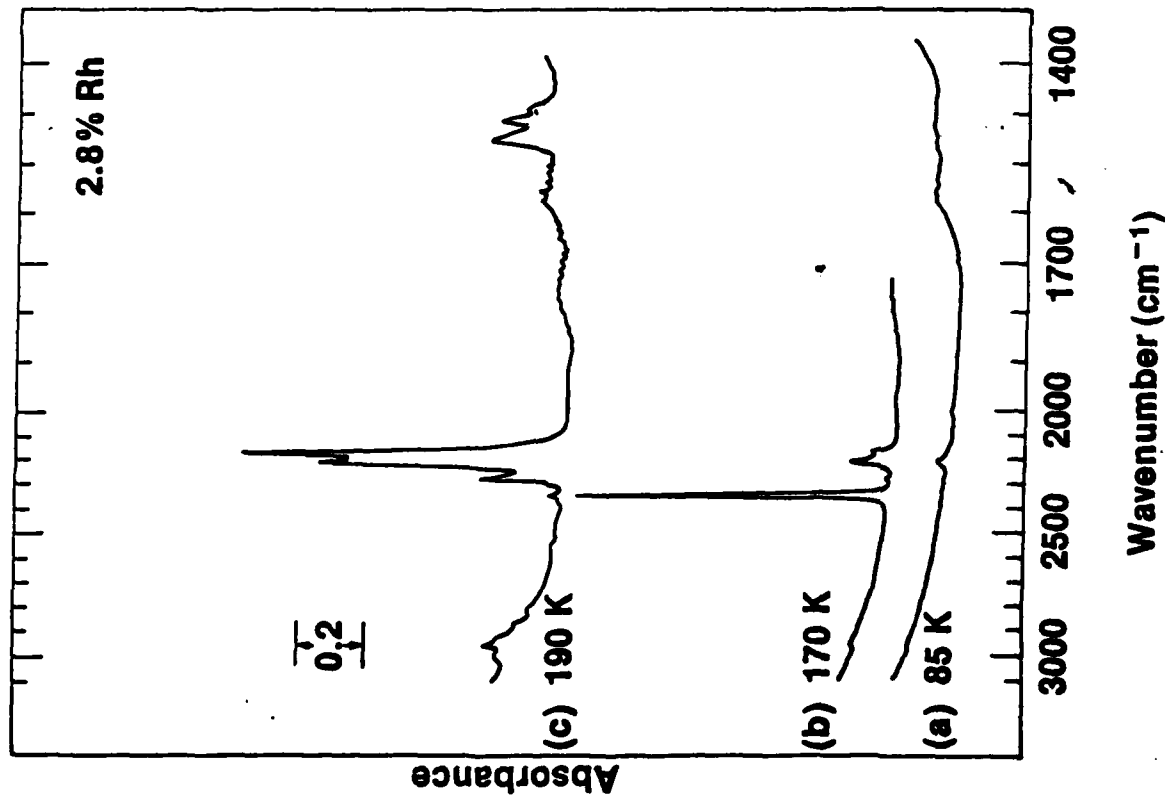
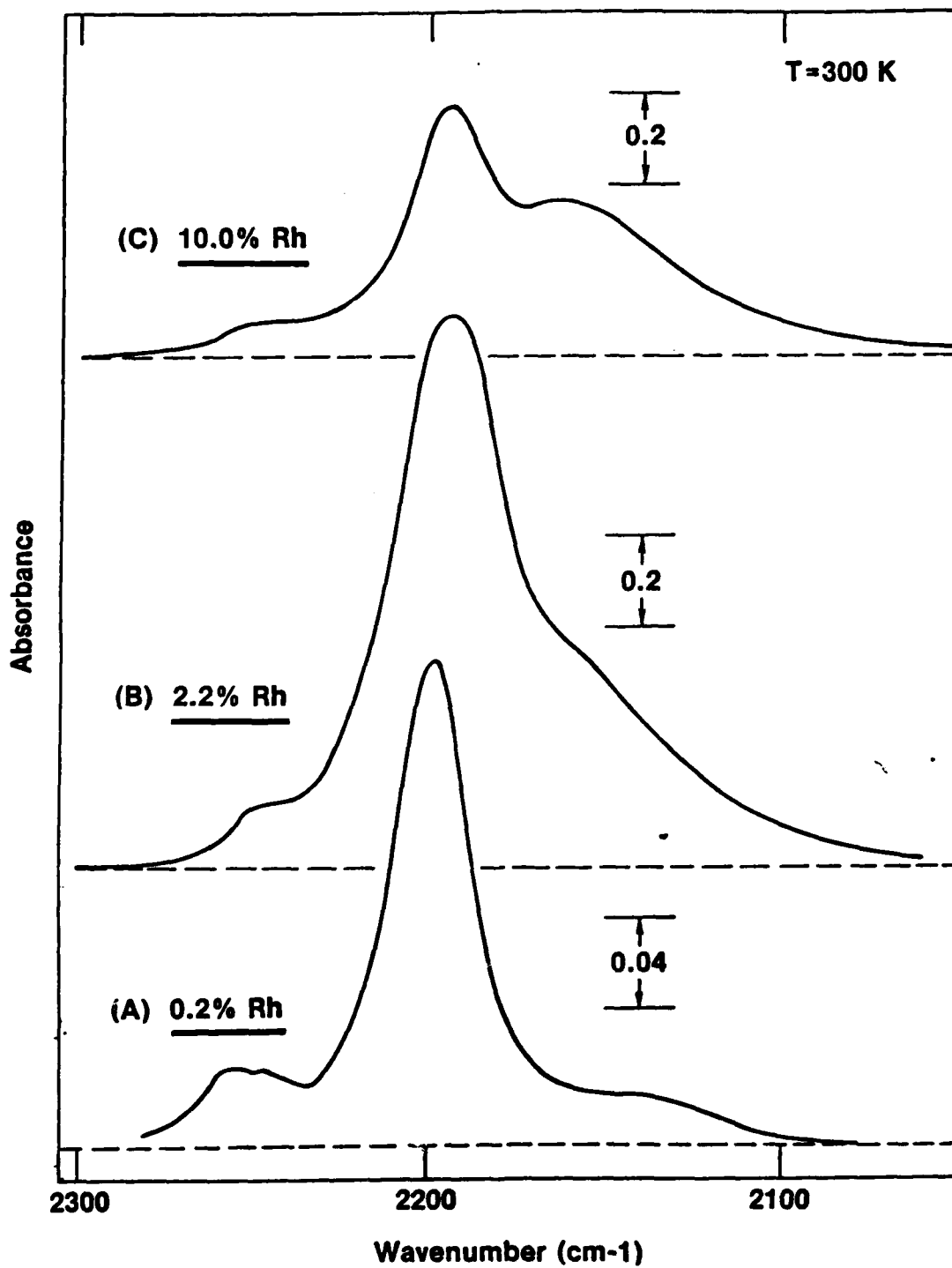


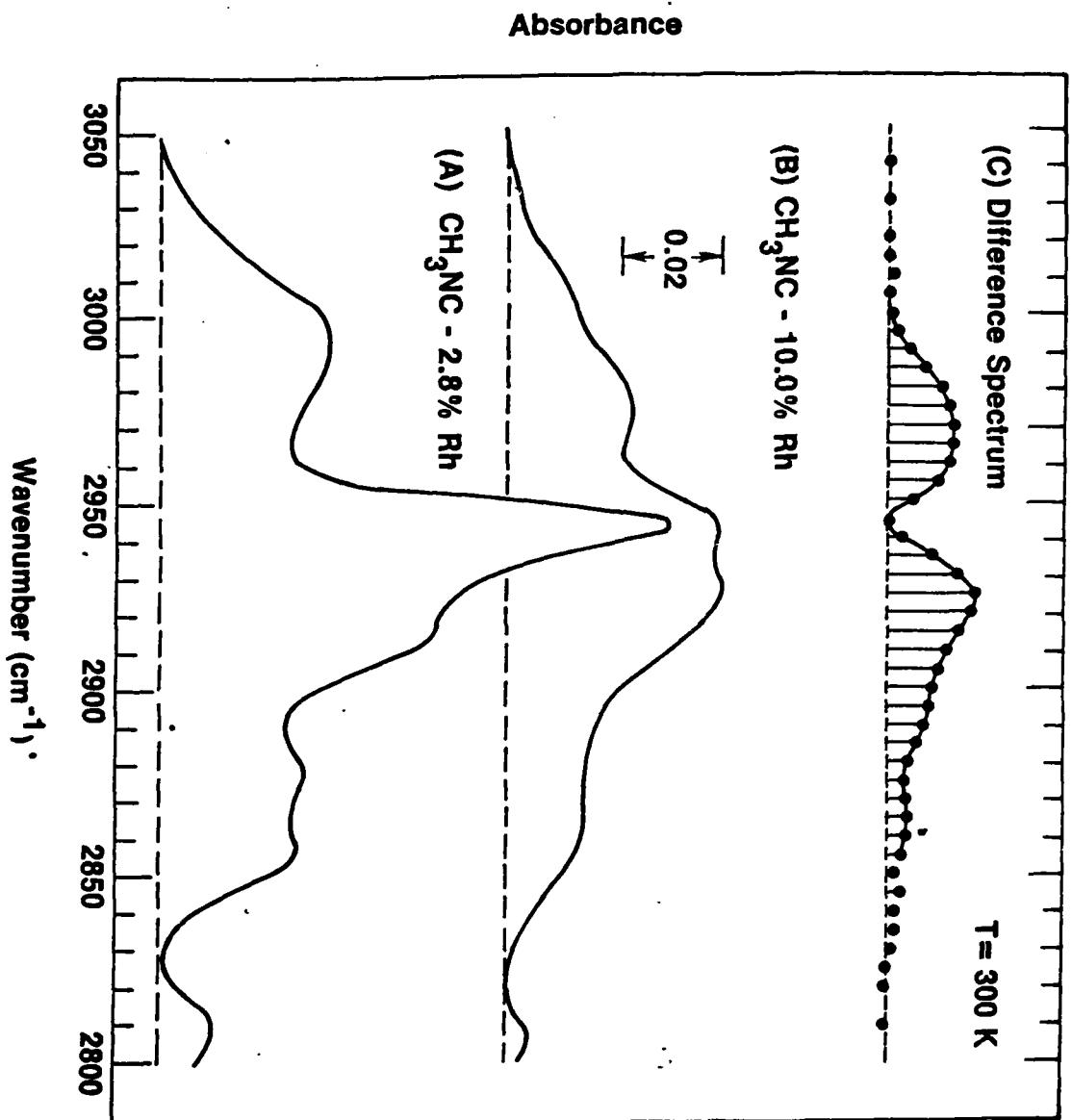
Figure 5

**Infrared Spectrum of  $\text{C}\equiv\text{N}$  Stretch for  $\text{CH}_3\text{NC}$   
Chemisorbed on  $\text{Rh}/\text{Al}_2\text{O}_3$ : Metal Dispersion Dependence**



**Figure 6**

Infrared Spectrum of  $\text{CH}_3$  Stretching Mode for Chemisorbed  
 $\text{CH}_3\text{NC}$  on  $\text{Rh}/\text{Al}_2\text{O}_3$ : Metal Dispersion Dependence



**Infrared Spectrum of CH<sub>3</sub> Bending Features:  
CH<sub>3</sub>NC Chemisorbed on Rh/Al<sub>2</sub>O<sub>3</sub>**

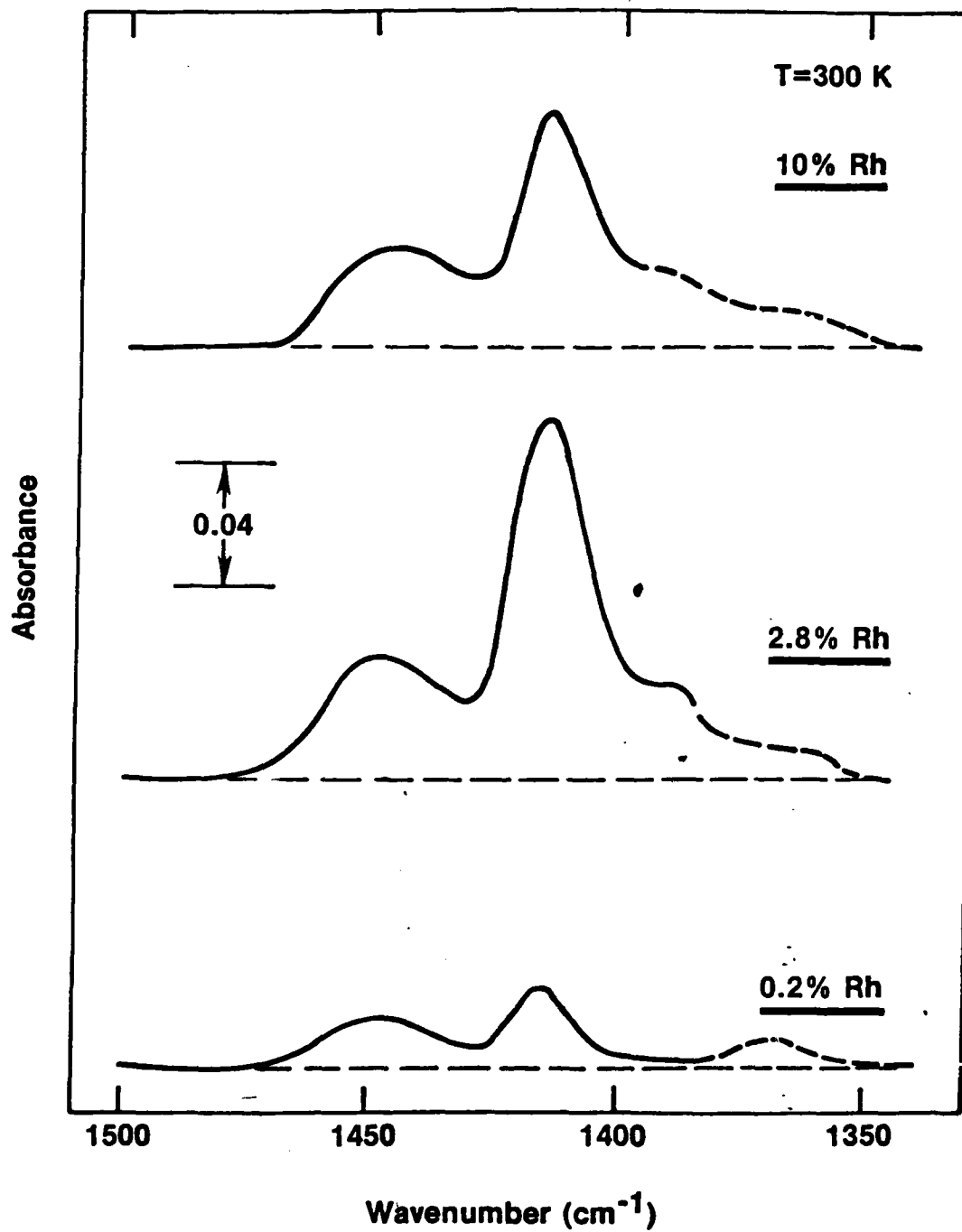


Figure 8

# Chemisorption of CO on CH<sub>3</sub>CN Saturated Rh/Al<sub>2</sub>O<sub>3</sub>

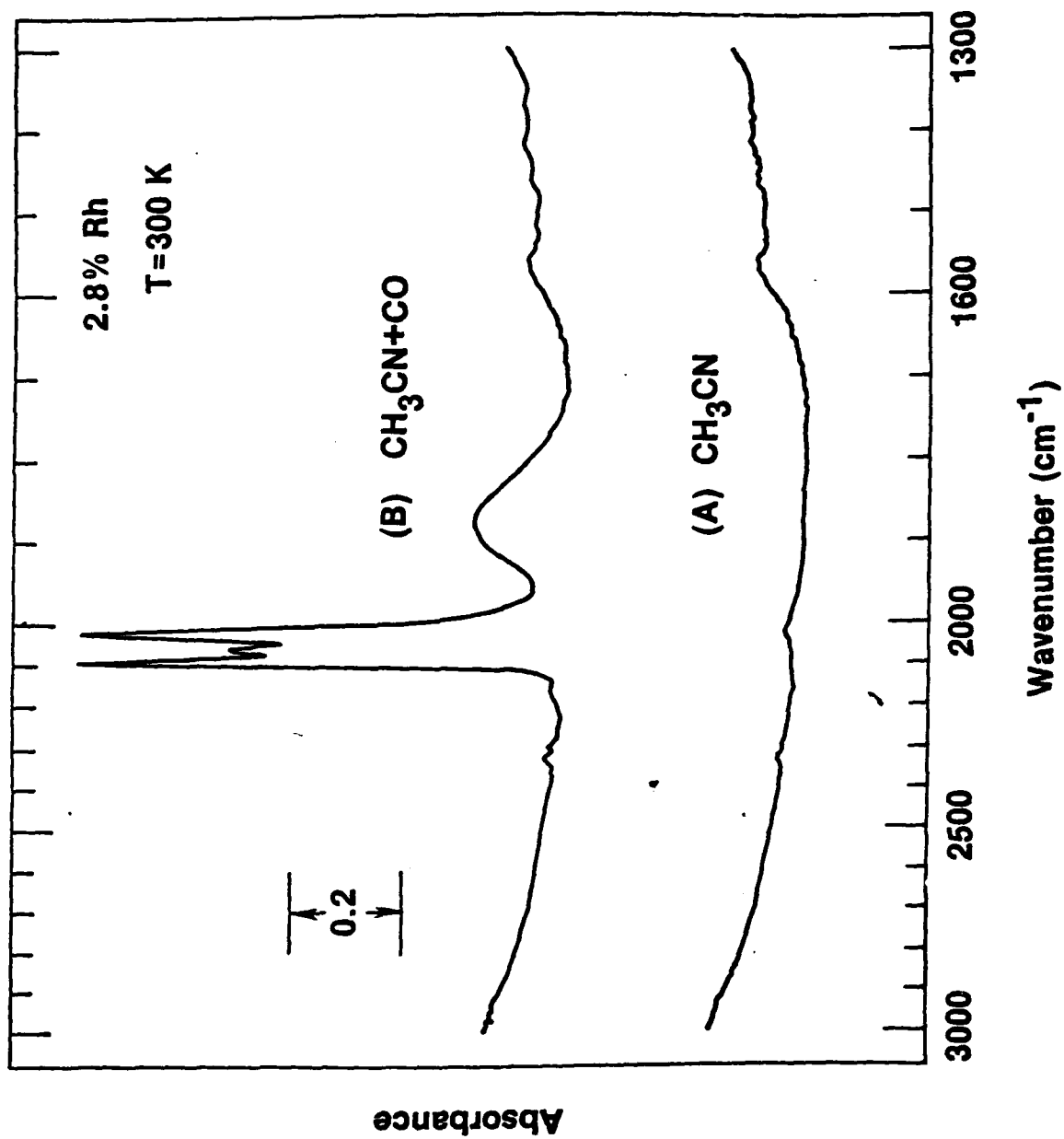


Figure 9